Vol 466|15 July 2010|doi:10.1038/nature09216

LETTERS

Diamonds sampled by plumes from the core–mantle boundary

Trond H. Torsvik[1,2,3], Kevin Burke[3,4], Bernhard Steinberger[1,2,5], Susan J. Webb[3] & Lewis D. Ashwal[3]

Diamonds are formed under high pressure more than 150 kilometres deep in the Earth's mantle and are brought to the surface mainly by volcanic rocks called kimberlites. Several thousand kimberlites have been mapped on various scales[1–4], but it is the distribution of kimberlites in the very old cratons (stable areas of the continental lithosphere that are more than 2.5 billion years old and 300 kilometres thick or more[5]) that have generated the most interest, because kimberlites from those areas are the major carriers of economically viable diamond resources. Kimberlites, which are themselves derived from depths of more than 150 kilometres, provide invaluable information on the composition of the deep subcontinental mantle lithosphere, and on melting and metasomatic processes at or near the interface with the underlying flowing mantle. Here we use plate reconstructions and tomographic images to show that the edges of the largest heterogeneities in the deepest mantle, stable for at least 200 million years and possibly for 540 million years, seem to have controlled the eruption of most Phanerozoic kimberlites. We infer that future exploration for kimberlites and their included diamonds should therefore be concentrated in continents with old cratons that once overlay these plume-generation zones at the core–mantle boundary.

Kimberlites are volatile-rich, potassic, ultramafic igneous rocks that vary enormously in chemical and isotopic composition, mineralogy and texture, and show evidence that they are derived from depleted, enriched and/or fertile mantle sources. The minimum depth of kimberlite generation, as inferred from diamond stability and experimental petrology, is about 150 km (refs 6 and 7), but some have suggested far deeper generation depths of 400–600 km (ref. 8) or even more than 660–1,700 km (refs 9 and 10). Here we put these results into wider perspective by demonstrating that most kimberlites generated during the past 540 million years (Myr) are probably related to plumes that had risen from the two plume generation zones[11] (PGZs) at the core–mantle boundary (CMB).

Large igneous provinces consist mainly of basaltic rock erupted relatively rapidly (in the course of 1–5 Myr) over great areas ($1–10 \times 10^6$ km^2; ref. 12). Earlier work has shown that most large igneous provinces of the past 300 Myr (when rotated back to their eruption sites) and active deep-plume-sourced hotspots at the Earth's surface (Fig. 1) project radially down to lie on narrow, stable PGZs at the CMB at the edge of the hot and dense large low-shear-wave-velocity provinces (LLSVPs[13]) of the deep mantle[11,14–19], thus demonstrating the long-term stability of LLSVPs. The 1% low-velocity contour in the lowermost layer of the SMEAN tomography model[20] is a reasonable proxy for the PGZs, because most reconstructed large igneous province eruption sites and steep horizontal gradients in shear-wave anomalies in the SMEAN model fall close to that contour[14]. In Fig. 1 we show 12 hotspots that have been found, by seismic tomography[18], to be sourced by deep plumes. There is evidence from other selection criteria that some further hotspots (for example, Tristan da Cunha, Réunion, Afar and Hawaii) are also sourced from deep plumes; these are not shown on our map, but they are also almost vertically above the PGZs[14,16].

To find out whether kimberlites show an association with PGZs similar to that shown by large igneous provinces and hotspots, we used plate reconstructions[21,22] to rotate kimberlites that are younger than the initial assembly of Pangaea (~320 Myr) to their original eruption sites. We find that 80% of kimberlites (1,112 out of 1,395) of the past 320 Myr were erupted when their eruption sites lay above a half-width of 15° on either side of the 1% slow contour of the SMEAN model in the lowermost mantle beneath Africa (Fig. 1). On average, this dominant part of the kimberlite population plots at a distance of 7 ± 5° from that contour (Supplementary Table 1). The most anomalous kimberlites younger than 320 Myr (17%) are in the Slave Province of Canada (Late Cretaceous/Early Tertiary period kimberlites[2]), which was close to a tectonically active continental margin at the time of their eruption.

A remarkable pattern is observed when we plot kimberlites on our series of plate reconstructions. At practically all times, eruption sites

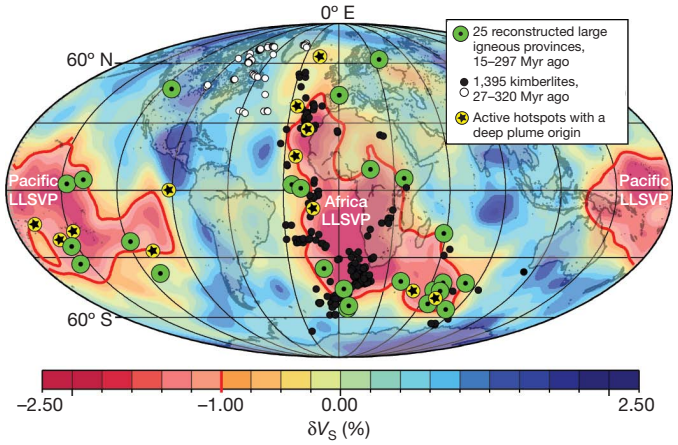

Figure 1 | Reconstructed large igneous provinces and kimberlites for the past 320 Myr with respect to shear-wave anomalies at the base of the mantle. The deep mantle (2,800 km on the SMEAN tomography model[20]) is dominated by two LLSVPs beneath Africa and the Pacific. The 1% slow contour (approximating to the PGZs) is shown as a thick red line. 80% of all reconstructed kimberlite locations (black dots) of the past 320 Myr erupted near or over the sub-African PGZ. The most 'anomalous' kimberlites (17%) are from Canada (white dots). Present-day continents are shown as a background, to illustrate the distribution of hotspots classified as being of deep-plume origin[18] and present-day shear-wave velocity anomalies (percentage δv_S), and bear no geographical relationship to reconstructed kimberlites or large igneous provinces.

[1]Physics of Geological Processes and Geosciences, University of Oslo, Blindern, 0316 Oslo, Norway. [2]Centre for Geodynamics, Geological Survey of Norway, Leiv Eirikssons vei 39, 7491 Trondheim, Norway. [3]School of Geosciences, University of the Witwatersrand, Wits 2050, South Africa. [4]Department of Geosciences, University of Houston, 312 Science and Research 1, Houston, Texas 77204-5007, USA. [5]Helmholtz Centre Potsdam, German Research Centre for Geosciences, 14473 Potsdam, Germany.

©2010 Macmillan Publishers Limited. All rights reserved

plot close to the African PGZ (Fig. 2 and Supplementary Figs 2–5). For the past 320 Myr, Gondwana, with Africa at its heart, has drifted slowly northward over the African PGZ (Supplementary Figs 2–5), and this readily explains the dominance of African (Gondwanan) kimberlites in the global record if, as we suggest, their origin relates to heat from deep plumes. Globally, kimberlite activity peaked between 70 and 120 Myr ago (Supplementary Fig. 1), corresponding to the time of formation of some of the most economically viable diamond sources in southern Africa. This time interval overlaps with the most intense large igneous province activities in the Earth's history, and also with a major superchron[9] of the magnetic field (~83–120 Myr ago; Cretaceous Normal Superchron). Almost 25% of all known kimberlites erupted between 80 and 90 Myr ago, when Africa was moving very slowly (~1 cm yr^{-1}) northeastward with respect to the mantle (Supplementary Fig. 1).

There are few Phanerozoic kimberlites with ages older than 320 Myr; only about 200 are known to have erupted between 540 and 320 Myr ago, and kimberlites were altogether absent from core Gondwana between 370 and 500 Myr ago. Plate reconstructions provide a possible reason for this: over this time interval, Gondwana was centred on the South Pole, and the bulk of the continent was located between, not over, the two LLSVPs and their marginal PGZs. By the late Devonian period (Fig. 3) Gondwana stretched from the South Pole (by then in South Africa) to the equator, and kimberlites started to erupt along the equatorial and eastern rim of Gondwana (by then in Australia). At this time, kimberlites with economically important diamonds also erupted on the Siberian continent (in Yakutsk; 344–376 Myr ago (refs 2, 23 and 24)). If the stability of LLSVPs and the eruption of large igneous provinces above their margins extend further back than 320 Myr ago, we can constrain Gondwana in longitude at 510 Myr ago and Siberia at 360 Myr ago by placing the Late Cambrian period Kalkarindji large igneous province in Australia and the Yakutsk large igneous province above the LLSVP margins (Fig. 4). In this reconstruction, kimberlites in Siberia between 350 and 360 Myr ago and in Gondwana (the part that became southern Africa) between 500 and 510 Myr ago (Fig. 3) erupted close to vertically above the African PGZ. Going further back, we can show that Cambrian kimberlites with economically important diamonds (535–542 Myr ago (ref. 25)) in Canada fall near the Pacific PGZ, whereas contemporaneous diamond-bearing kimberlites in South Africa erupted above the African PGZ (Fig. 4). Using the principles of plate tectonics and the Yakutsk and Kalkarindji large igneous provinces to calibrate our global reconstruction in longitude, we generated semi-absolute reconstructions for the entire Lower and Middle Palaeozoic era, and plotted kimberlite distributions from the major kimberlite-bearing continents (Laurentia, Siberia and Gondwana). These reconstructions show that all kimberlites that erupted between 341 and 542 Myr ago lay, at their times of eruption, above the African (Siberia,

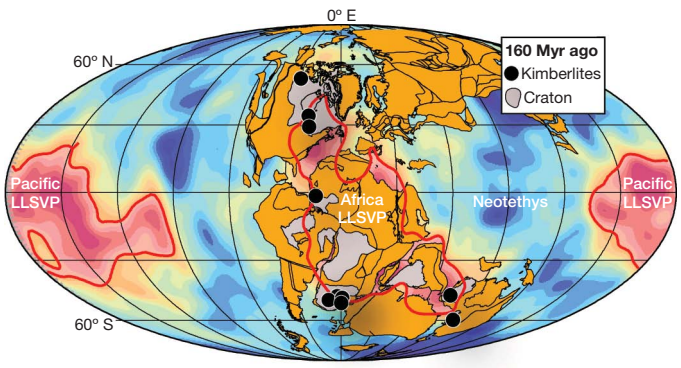

Figure 2 | Late-Jurassic plate reconstruction of continents and kimberlite locations draped on the SMEAN model. We reconstructed kimberlite locations with eruption ages between 155 and 165 Myr ago to the average of 160 Myr ago. Reconstructed kimberlite locations are found near the edges of the African LLSVP (near the 1% slow contour, which is shown as a thick red line) and at the old cratons in North America[4], northwestern Africa, South Africa (the Kalahari craton[1]) and Australia[30]. The most important cratons for kimberlite eruption since the Carboniferous period are shaded in grey.

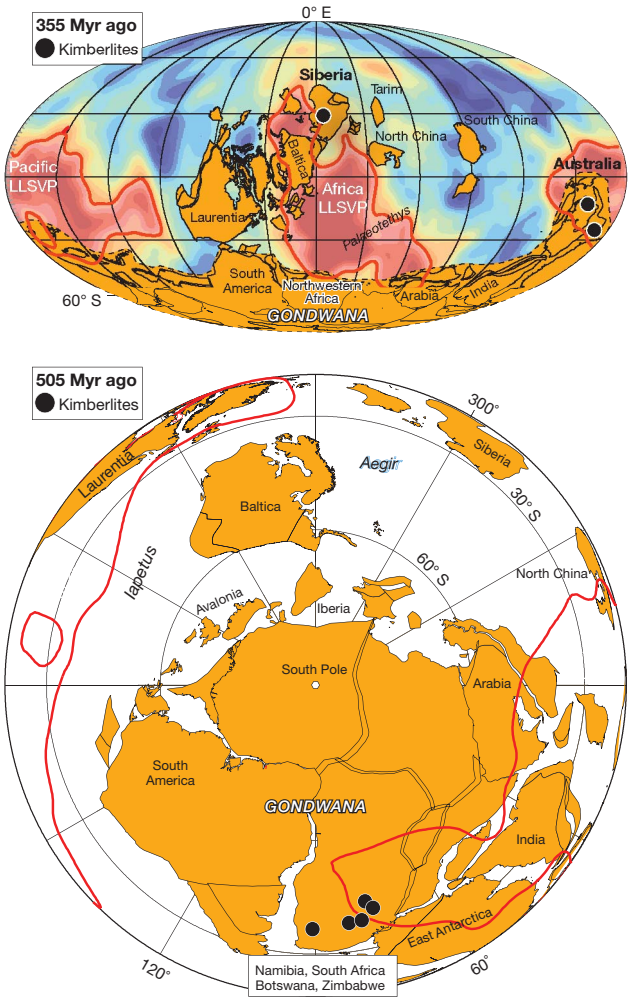

Figure 3 | Devonian and Cambrian period plate reconstructions draped on the SMEAN model. We reconstructed kimberlite locations with eruption ages between 350 and 360 Myr ago to the average of 355 Myr ago, and ages between 500 and 510 Myr ago to the average of 505 Myr ago; they all fall close to vertically above the SMEAN model −1% contours (PGZs), shown as thick red lines.

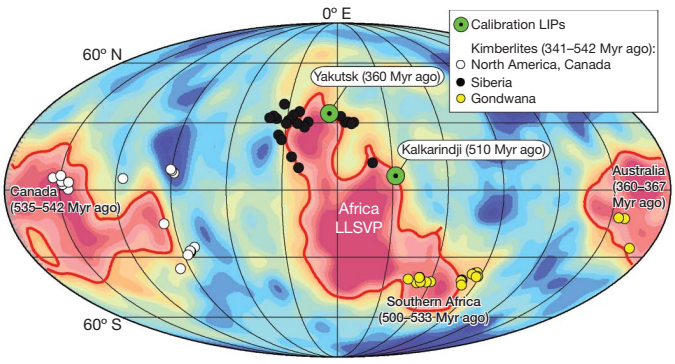

Figure 4 | Reconstructed Palaeozoic kimberlites from Laurentia (North America, Canada), Siberia and core Gondwana draped on the SMEAN model. The SMEAN model -1% contour is shown as a thick red line.

©2010 Macmillan Publishers Limited. All rights reserved

southern Africa) and Pacific (Laurentia, Australia) PGZs (Figs 3 and 4). On average, those kimberlites plot at a distance of $8 \pm 4^\circ$ from the 1% slow contour of the SMEAN model, with 93% lying within a half-width of 10° from that contour (Supplementary Table 1).

Mantle plumes have been argued, using a variety of observations[9,10,23,26], to be important in some or all kimberlite eruptions. We have shown that large igneous provinces and hotspot volcanoes develop from the deep-seated mantle plumes that rose from two PGZs[11,14–16]. Here, for the first time, we show that plumes that have risen from the PGZs at the margins of the sub-African (Figs 1 and 2 and Supplementary Figs 2–6) and the Pacific (Figs 3 and 4) LLSVPs were also involved in kimberlite eruption. This clustering of kimberlites above LLSVP margins is extremely unlikely to be the result of chance, and we estimate that it has a probability of 0.1–1% or less (Supplementary Figs 7 and 8).

Kimberlites are only known within continents, and about 80% of those that have erupted during the past 320 Myr formed within a part of a continent that at the time of the eruption lay close to vertically above a PGZ at the CMB (Fig. 1). The high concentration of economically viable kimberlites in Africa is due to the very old (>2.5 billion years) cratonic parts of the continent lying above a PGZ at various times during the past 320 Myr. This indicates that the search for kimberlites and the diamonds that they contain might be profitably concentrated in areas within the old cratons of continents that once overlay a PGZ (Fig. 2 and Supplementary Figs 2–6). Current limitations in absolute plate reconstructions make it harder to identify such places for times earlier than 320 Myr ago (ref. 16). However, if the relationship of large igneous province and kimberlite eruptions to the PGZs holds true for that time (Figs 3 and 4), we can use the information to position continents close to their original longitude long before the assembly of Pangaea and probably throughout the entire Phanerozoic eon.

We can now show that three distinct kinds of igneous bodies, represented by (1) at least 12 active hotspot volcanoes[18], (2) 23 large igneous provinces of the past 300 Myr (refs 11 and 14–16) and (3) 1,112 kimberlites from the past 320 Myr (this paper) now lie, in the case of the active hotspot volcanoes, or lay at the time of their eruption, in the cases of large igneous provinces and kimberlites, vertically or nearly vertically above a PGZ at the CMB (Fig. 1). The PGZs can be described as narrow loci of an intermittent or continuous upward flux of hot and buoyant material from the CMB. Lateral flow above the CMB may be deflected upwards at the margins of LLSVPs, which are probably chemically distinct[11,13–17]. This flux appears to be related to the emplacement of large igneous provinces, 'hotspot volcanoes' (of which some, but not all, may lie on tracks that originated in large igneous provinces) and kimberlites.

Large igneous provinces and kimberlites have erupted since Archaean times. Our results show that most of these rocks have been derived from deep plumes originating at the margins of LLSVPs, but whether the African and Pacific LLSVPs have remained in the same places throughout the Earth's history is less certain[16,27,28]. The stability of LLSVPs in their present locations at the CMB can be demonstrated for large igneous provinces and kimberlites for the past 320 Myr. Most large igneous provinces and kimberlites erupted during roughly the past 200 Myr, so we can be confident about LLSVP stability since then. Explaining those stable LLSVPs and the rising of plumes from their edges requires a new and challenging generation of dynamic mantle models[29]. We can find a reasonable plate reconstruction with continents placed in a longitude such that the two known large igneous provinces and roughly 200 kimberlites that erupted between 540 and 320 Myr ago fall close to vertically above the present LLSVP margins. This indicates that the near-antipodal locations of the two existing LLSVPs on the equator may have been stationary for as much as 540 Myr, and thus seem to be insensitive to surface plate motions, including those of the formation of Pangaea.

METHODS SUMMARY

We combined reconstructions derived from a hotspot frame for the past 100 Myr with a palaeomagnetic frame dating back to the initial assembly of Pangaea (320 Myr ago). This is known as the global hybrid frame[21], which we correct here for true polar wander[22] between 320 and 100 Myr ago. For data earlier than 320 Myr ago we used the PGZ-reconstruction method to calibrate longitudes[16]. This method uses the long-term relationship between large igneous provinces and PGZs to estimate longitudes for large igneous provinces, and we use it here to identify the continents under which the PGZs lay at times of kimberlite eruption. We calibrated longitudes more than 320 Myr ago by placing the Yakutsk large igneous province in Siberia (~360 Myr ago) and the Kalkarindji large igneous province in Australia/Gondwana (~510 Myr ago) over the most likely edges of the African LLSVP[16] (Fig. 4). We know the palaeolatitude for the Yakutsk (~35° N) and Kalkarindji (~9° N) large igneous provinces from palaeomagnetic data from Siberia and Gondwana.

We derived the kimberlite locations from numerous sources (including a recent African compilation[3]), and included 1,395 'dated' kimberlites for the past 320 Myr. Kimberlite age control varies from excellent (for example, U/Pb dating) to less certain (that is, ages assumed to be similar to those of neighbouring kimberlites). We did not include undated kimberlites or those with vaguely described ages in our analysis. We first rotated each kimberlite site to southern African coordinates using relative rotation parameters[21], and then rotated them to their correct palaeoposition on the globe (Fig. 1) using the absolute reference frames outlined above. We then draped reconstructed kimberlite eruption sites (symbols in Figs 1–4 may represent multiple sites) on the present-day SMEAN-model anomalies near the CMB, assuming that the African and the Pacific LLSVPs have remained stationary for at least 300 Myr.

We produced diagrams with GMT (gmt.soest.hawaii.edu), GMAP (www.geodynamics.no) and GPlates (www.gplates.org) software, and with SPlates software developed for our industry sponsor (Statoil).

Full Methods and any associated references are available in the online version of the paper at www.nature.com/nature.

Received 21 September 2009; accepted 19 May 2010.

1. Jelsma, H. A. *et al.* Preferential distribution along transcontinental corridors of kimberlites and related rocks of southern Africa. *S. Afr. J. Geol.* **107,** 301–324 (2004).
2. Kjarsgaard, B. A. in *Mineral Deposits of Canada: A Synthesis of Major Deposit-Types, District Metallogeny, the Evolution of Geological Provinces, and Exploration Methods* (ed. Goodfellow, W. D.) 245–272 (Geol. Assoc. Canada Special Publication 5, 2007).
3. Jelsma, H., Barnett, W., Richards, S. & Lister, G. Tectonic setting of kimberlites. *Lithos* **112,** 155–165 (2009).
4. Heaman, L. M. & Kjarsgaard, B. A. Timing of eastern North American kimberlite magmatism: continental extension of the Great Meteor hotspot track? *Earth Planet. Sci. Lett.* **178,** 253–268 (2000).
5. Jordan, T. H. in *The Mantle Sample: Inclusions in Kimberlites and Other Volcanics* (eds Boyd, F. R. &. Meyer, H. O. A.) 1–14 (AGU, 1979).
6. Mitchell, R. H. *Kimberlites: Mineralogy, Geochemistry and Petrology* (Plenum, 1986).
7. Wyllie, P. J. The origin of kimberlites. *J. Geophys. Res.* **85,** 6902–6910 (1980).
8. Ringwood, A. E., Kesson, S. E., Hibberson, W. & Ware, N. Origin of kimberlites and related magmas. *Earth Planet. Sci. Lett.* **113,** 521–538 (1992).
9. Haggerty, S. E. A diamond trilogy: superplumes, supercontinents, and supernovae. *Science* **285,** 851–861 (1999).
10. Hayman, P. C., Kopylova, M. G. & Kaminsky, F. V. Lower mantle diamonds from Rio Soriso (Juina area, Mato Grosso, Brazil). *Contrib. Mineral. Petrol.* **149,** 430–445 (2005).
11. Burke, K., Steinberger, B., Torsvik, T. H. & Smethurst, M. A. Plume generation zones at the margins of large low shear velocity provinces on the core–mantle boundary. *Earth Planet. Sci. Lett.* **265,** 49–60 (2008).
12. Bryan, S. & Ernst, R. Revised definition of large igneous provinces (LIPs). *Earth Sci. Rev.* **86,** 175–202 (2008).
13. Garnero, E. J., Lay, T. & McNamara, A. K. in *Plates, Plumes, and Planetary Processes* (eds Foulger, G. R. & Jurdy, D. M.) 79–109 (Geol. Soc. Am. Special Paper 430, 2007).
14. Torsvik, T. H., Smethurst, M. A., Burke, K. & Steinberger, B. Large igneous provinces generated from the margins of the large low-velocity provinces in the deep mantle. *Geophys. J. Int.* **167,** 1447–1460 (2006).
15. Torsvik, T. H., Smethurst, M. A., Burke, K. & Steinberger, B. Long term stability in deep mantle structure: evidence from the ~300 Ma Skagerrak-centered large igneous province (the SCLIP). *Earth Planet. Sci. Lett.* **267,** 444–452 (2008).
16. Torsvik, T. H., Steinberger, B., Cocks, L. R. M. & Burke, K. Longitude: linking Earth's ancient surface to its deep interior. *Earth Planet. Sci. Lett.* **276,** 273–283 (2008).
17. Thorne, M. S., Garnero, E. J. & Grand, S. Geographic correlation between hot spots and deep mantle lateral shear-wave velocity gradients. *Phys. Earth Planet. Inter.* **146,** 47–63 (2004).

©2010 Macmillan Publishers Limited. All rights reserved

18. Montelli, R., Nolet, G., Dahlen, F. & Masters, G. A catalogue of deep mantle plumes: new results from finite-frequency tomography. *Geochem. Geophys. Geosyst.* **7,** Q11007, doi: 10.1029/2006GC001248 (2006).
19. Davaille, A., Stutzmann, E., Silveira, G., Besse, J. & Courtillot, V. Convective patterns under the Indo-Atlantic. *Earth Planet. Sci. Lett.* **239,** 233–252 (2005).
20. Becker, T. W. & Boschi, L. A comparison of tomographic and geodynamic mantle models. *Geochem. Geophys. Geosyst.* **3,** 1003, doi: 10.1029/2001GC000168 (2002).
21. Torsvik, T. H., Müller, R. D., Van der Voo, R., Steinberger, B. & Gaina, C. Global plate motion frames: toward a unified model. *Rev. Geophys.* **46,** RG3004, doi: 10.1029/2007RG000227 (2008).
22. Steinberger, B. & Torsvik, T. H. Absolute plate motions and true polar wander in the absence of hotspot tracks. *Nature* **452,** 620–623 (2008).
23. Yakubchuk, A. Diamond deposits of the Siberian craton: products of post-1200 Ma plume events affecting the lithospheric keel. *Ore Geol. Rev.* **35,** 155–163 (2009).
24. Kinny, P. D., Griffin, B. J., Heaman, L. M., Brakhfogel, F. F. & Spetsius, Z. V. Shrimp U–Pb ages of perovskite from Yakutian kimberlites. *Russ. Geol. Geophys.* **38,** 97–105 (1997).
25. Heaman, L. M., Kjarsgaard, B. A. & Creaser, R. A. The timing of kimberlite magmatism in North America: implications for global kimberlite genesis and diamond exploration. *Lithos* **71,** 153–184 (2004).
26. Le Roex, A. P., Bell, D. R. & Davis, D. Petrogenesis of group I kimberlites from Kimberley, South Africa: evidence from bulk-rock geochemistry. *J. Petrol.* **44,** 2261–2286 (2003).
27. Zhong, S., Zhang, N., Li, Z. X. & Roberts, J. H. Supercontinent cycles, true polar wander, and very long-wavelength mantle convection. *Earth Planet. Sci. Lett.* **261,** 551–564 (2007).
28. Li, Z. X. & Zhong, S. Supercontinent–superplume coupling, true polar wander and plume mobility: plate dominance in whole-mantle tectonics. *Phys. Earth Planet. Inter.* **176,** 143–156 (2009).
29. Tan, E., Leng, W., Zhong, S. & Gurnis, M. On the fixity of the thermo-chemical piles at the base of mantle. *Eos (Fall Meeting)* ***90,*** abstr. DI12A–08 (2009).
30. Jaques, A. L. Kimberlite and lamproite diamond pipes. *AGSO J. Aust. Geol. Geophys.* **17,** 153–162 (1998).

Supplementary Information is linked to the online version of the paper at www.nature.com/nature.

Acknowledgements We thank R. Trønnes, S. Haggerty, M. Gurnis and C. Gaina for comments and discussions, and S. King and D. Evans for reviews. We acknowledge Statoil and the Norwegian Research Council for financial support.

Author Contributions T.H.T. and K.B. developed the conceptual idea for the study, B.S. developed statistical methods and tests and S.J.W. and L.D.A. assembled input data. All authors contributed to discussions and writing of the manuscript.

Author Information Reprints and permissions information is available at www.nature.com/reprints. The authors declare no competing financial interests. Readers are welcome to comment on the online version of this article at www.nature.com/nature. Correspondence and requests for materials should be addressed to T.H.T. (trond.torsvik@ngu.no).

©2010 Macmillan Publishers Limited. All rights reserved

METHODS

Our methods depend on several factors, including kimberlite age uncertainties and the choice of both plate and tomography models. In addition, plume sources may have been advected in the mantle[31,32], and a kimberlite eruption site may not mark precisely where a plume impinged on the base of the lithosphere, but rather the location of material that may have propagated horizontally within the lithosphere from a plume[11,33,34,14]. The observation that kimberlites in some cases occur in clusters or lines[3] may indicate that their surface distribution is partly structurally controlled; it is therefore complex to estimate the net effect of these individual sources of uncertainty.

We have previously examined nine different shear-wave-velocity models; they all provide broadly similar characteristics near the CMB, so the choice of tomographic model is not critical to our conclusions[11,16] but may lead to slightly different statistical correlations. As an example, we compare the 1% slow contour of the SMEAN model with the 0.96% slow contour in the Castle *et al.* D″ model[35] and the 0.77% slow contour in the Kuo *et al.* D″ model[36] (Supplementary Fig. 6), both of which globally, at the CMB, approximately correspond to the 1% slow contour of the SMEAN model[11]. Twenty-five reconstructed large igneous provinces plot on average at a distance of $8 \pm 9^\circ$ (mean $\pm$ standard deviation) from the SMEAN model contour, whereas the distances from the CASTLE and KUO contours are reduced to $5 \pm 3^\circ$ and $6 \pm 4^\circ$ (Supplementary Table 1). In the SMEAN model, 80% of all reconstructed large igneous provinces plot within a 10° half-width centred on the 1% slow contour, increasing to 96% for the CASTLE contour (Supplementary Table 1 and Supplementary Fig. 7a). The CASTLE model scores the highest because its contour contains two small subareas at the CMB that plot near the Siberian Traps and the Columbia River Basalt (ST and CB in Supplementary Fig. 6). The CASTLE contour is also continuous further north in the North Atlantic, and thus the Iceland hotspot (Fig. 1) also fits this model best. We consider it likely that the Iceland plume is related to a continuation of the Africa LLSVP, and it is possible that the smaller anomaly now underlying the reconstructed Siberia Trap has also been part of the African LLSVP. Different tomography models therefore do matter in a statistical sense, but all three models (and most other models at the CMB[11,16]) demonstrate that large igneous provinces correlate with the edges of CMB heterogeneities and never with their centres.

Kimberlite distribution is also sensitive to the specific tomography model, but the roughly 17% of 'anomalous' Late-Cretaceous–Early-Tertiary North American kimberlites in the database of the last 320 Myr (~12% of the entire Phanerozoic collection) are anomalous in all models. The remaining kimberlites plot at an average distance of $7 \pm 4^\circ$ from the SMEAN model contour, $6 \pm 4^\circ$ from the CASTLE contour and $3 \pm 3^\circ$ from the KUO contour (Supplementary Table 1; 27–314 Myr population). Seventy-three per cent plot within 10° of the SMEAN model contour (Supplementary Fig. 7c). That increases to 85% and 94% for the CASTLE and KUO contours. For comparison, *in-situ* (that is, non-reconstructed) kimberlite locations plot at a distance of $19 \pm 12^\circ$ with only 14% inside the 10° band of the SMEAN model—clearly a much worse fit (Supplementary Fig. 7b). Although we appreciate the better fit for the CASTLE and KUO models, these contours are longer, and hence the area within 10° is larger than for the SMEAN model −1% contour. However, the major reason that the KUO model best fits the kimberlite data (Supplementary Table 1) is that a large population of 80–90-Myr-old kimberlites in South Africa (white arrows marked 2 in Supplementary Fig. 6; see also Supplementary Fig. 4) plot right on top of the 0.77% slow KUO contour, whereas they plot at some distance inside the SMEAN model contour.

An absolute plate motion model must account for the distribution of subducted slab material in the mantle through geological time. Such a reference system, based on information about subducted slabs identified from seismic tomography and plate kinematic models, is still in its infancy, but as a plate model sensitivity test we reconstructed kimberlite eruption sites for the past 300 Myr using the subduction reference frame of van der Meer *et al.*[37]. Excluding the Late Cretaceous/Early Tertiary North American kimberlites, kimberlites plot at a distance of $9 \pm 4^\circ$, with 65% inside the 10° band for the SMEAN model (Supplementary Fig. 7c). This is slightly worse, but within the error of our hybrid plate model.

We have previously given a statistical argument that the coincidence of reconstructed large igneous provinces with the LLSVP margins is extremely unlikely to have resulted from pure chance[11], but how likely is it that a kimberlite distribution near the LLSVP edges occurs by chance? Kimberlites only occur in continents, and the diamond-bearing kimberlites occur in cratons more than 2.5 billion years old. Those old cratons make up roughly 15% of the total area of the continents. In Supplementary Fig. 7d, we plot the fraction of cratons that are within 10° of the PGZ as a function of time, on the basis of three tomography models (SMEAN, CASTLE and KUO). This should be equal to the fraction of kimberlites if they were formed randomly on the cratons. For comparison, 62% (dashed red line) of all kimberlites (980 of 1,588) and 33% of the surface of the sphere are within 10° based on the SMEAN model. The percentage of kimberlites (62%) is slightly less than the maximum percentage of cratons (~70%) that are within 10° of the SMEAN model slow margin, but at the times when most of the kimberlites were formed a much smaller percentage of cratons were within 10°—about the same as, or even less than, the percentage of the entire surface of the sphere: that is, the result that would be expected if the cratons were placed randomly. This shows that the clustering of kimberlites near the 1% slow margin cannot be due to a clustering of cratons near the 1% slow margin. Numbers for the other tomography models, CASTLE and KUO, are slightly higher but lead to the same conclusion. At the time when most kimberlites formed, the cratons' location relative to the 1% slow margin was more or less as would be expected from a random distribution, but the kimberlites were not formed on the cratons in the way that would be expected in a random distribution. The lighter-coloured dashed lines show that the fraction of kimberlites within 10° of the PGZs decreases if we restrict ourselves to more recent times. This may be partly an effect of less freedom in longitude adjustment for more recent times—we have in fact adjusted longitudes to fit large igneous provinces above PGZs before 320 Myr (Fig. 4). Hence, there may be an increasing bias towards an increased fraction of kimberlites above PGZs further back in time. Nevertheless, even for the most recent time interval, up to 130 Myr ago, in which longitudes can be constrained by hotspot tracks, the fraction of kimberlites within 10° of PGZs is much higher than the fraction of cratons, so the clustering of kimberlites near PGZs cannot be due to freedom in longitude. Although in our reconstruction we switch from a hotspot-based to a palaeomagnetic reference frame at 100 Myr ago, comparison of the two frames shows only a minor difference in longitude between 100 and 130 Myr ago.

The probability that kimberlites were emplaced randomly is further explored in Supplementary Fig. 8. The calculated probabilities are quite variable, depending on which tomography model is used (different colours), whether we consider the fraction of individual kimberlites within a half-width of 10° of the PGZs (lines) or the fraction of kimberlite 'groups' (filled circles), which time interval is considered and how many independent groups there are. Results further depend on the half-width and on which contour is used to define the PGZs (not shown).

Because groups with larger numbers of kimberlites should presumably be given more weight, we expect that the most appropriate estimate for probability in each case lies somewhere between the filled circles and the line of same colour in Supplementary Fig. 8. We estimate that there are about 43 to 55 'independent' groups of kimberlites that have formed in the last 542 Myr. As indicated in Supplementary Fig. 7d and Supplementary Table 1, we expect that with more tight, independent constraints on longitude more than 130 Myr ago, and especially more than 320 Myr ago, the fraction of kimberlites within 10° of the PGZs might be slightly, but not substantially, less; hence, probabilities might be slightly higher than those inferred from the range 43–55 in Supplementary Fig. 8. On the other hand, probability estimates from kimberlites younger than 320 Myr only are rather high, because during that time interval a large fraction of cratons was already within 10° of the PGZs. However, most kimberlites erupted at times when the fraction of cratons within 10° of the PGZs was much less, so these estimates are probably too high. Given all this, we expect that the probability of the distribution of kimberlites relative to PGZs being essentially random is about 0.1–1% or less. We emphasize that this estimate considers all kimberlites, including the 'anomalous' ones from Canada and the large cluster in South Africa, which is reconstructed above the African LLSVP away from its margin, if the SMEAN model 1% slow contour is used. We regard it as highly likely that the distribution of kimberlites is indeed related to the PGZs at the margins of LLSVPs in the lowermost mantle.

It has been suggested that kimberlite eruptions in, for example, North America and Africa occurred during periods of relatively slow continental motion[38]. To test this idea, we calculated the absolute motion of South Africa and North America for the past 320 Myr (Supplementary Fig. 1b). Our velocity curves differ from those of England and Houseman[38], but we notice that South Africa has relatively low speeds (1–3.5 cm yr^{-1}) during peaks in kimberlite eruption (70–100 Myr ago and 110– 120 Myr ago). These lows are also seen for North America, but there are two high-velocity spikes. The spike at 50–60 Myr ago is associated with 'anomalous' kimberlites (Fig. 1, white dots), erupted shortly after the collision of the ribbon continent of the Cordillera with North America, which was a time of tectonic activity in the Canadian Rockies when cracks that fostered decompression melting are likely to have formed in the Slave Province[39]. Only one lower-mantle mineral assemblage has been reported in Cretaceous–Tertiary kimberlites in Canada, but there is abundant majoritic garnet included in diamond[40,41]. A transition-zone (410–660 km) activated plume by 'large scale extension' seems to be a reasonable explanation for these 'anomalous' kimberlites.

That the reconstructed positions of at least 23 large igneous provinces, and now the majority of kimberlites (Fig. 1), all fall near the 1% slow contour demonstrates that the majority of both large igneous provinces and kimberlites are derived from the PGZs near the CMB. These observations are undoubtedly incompatible with passive plate-driven models for large igneous province

©2010 Macmillan Publishers Limited. All rights reserved

genesis[42], because in such alternative models there should be no correlation between surface volcanism and deep-mantle heterogeneities, nor is it very likely that upper mantle and crustal processes could affect the polarity pattern of the geodynamo (Supplementary Fig. 1).

31. Steinberger, B., Sutherland, R. & O'Connell, R. J. Prediction of Emperor–Hawaii seamount locations from a revised model of plate motion and mantle flow. *Nature* **430,** 167–173 (2004).
32. Boschi, L., Becker, T. W. & Steinberger, B. Mantle plumes: dynamic models and seismic images. *Geochem. Geophys. Geosyst.* **8,** Q10006, doi: 10.1029/2007GC001733 (2007).
33. Sleep, N. H. Mantle plumes from top to bottom. *Earth Sci. Rev.* **77,** 231–271 (2006).
34. Courtillot, V., Jaupart, C., Manighetti, I., Tapponnier, P. & Besse, J. On causal links between flood basalts and continental breakup. *Earth Planet. Sci. Lett.* **166,** 177–195 (1999).
35. Castle, J. C., Creager, K. C., Winchester, J. P. & van der Hilst, R. D. Shear wave speeds at the base of the mantle. *J. Geophys. Res.* **105,** 21543–21558 (2000).
36. Kuo, B.-Y., Garnero, E. J. & Lay, T. Tomographic inversion of *S–SKS* times for shear wave velocity heterogeneity in D'': degree 12 and hybrid models. *J. Geophys. Res.* **105,** 139–157 (2000).
37. van der Meer, D. G., Spakman, W., van Hinsbergen, D. J. J., Amaru, M. L. & Torsvik, T. H. Towards absolute plate motions constrained by lower-mantle slab remnants. *Nature Geosci.* **3,** 36–40 (2010).
38. England, P. & Houseman, G. On the geodynamic setting of kimberlite genesis. *Earth Planet. Sci. Lett.* **67,** 109–122 (1984).
39. Johnston, S. The Cordilleran ribbon continent of North America. *Annu. Rev. Earth Planet. Sci.* **36,** 495–530 (2008).
40. Davies, R., Griffin, W. L., O'Reilly, S. Y. & McCandless, T. E. Inclusions in diamonds from the K14 and K10 kimberlites, Buffalo Hills, Alberta, Canada: diamond growth in a plume? *Lithos* **77,** 99–111 (2004).
41. Stachel, T., Harris, J. W. & Muehlenbachs, K. Sources of carbon in inclusion bearing diamonds. *Lithos* **112,** 625–637 (2009).
42. Foulger, G. R. & Jurdy, D. M. (eds) *Plates, Plumes, and Planetary Processes* (Geol. Soc. Am. Special Paper 430, 2007).

©2010 **Macmillan Publishers Limited. All rights reserved**

SUPPLEMENTARY INFORMATION

Supplementary Information

We have also analyzed clusters of kimberlites on plate reconstructed maps in 10 Myr steps and Figures S2-5 show the results for the past 250 My with a focus on the Gondwana elements that constituted about half of the Pangea supercontinent. In this time range kimberlites are found in South Africa (notably on the Kalahari craton[1]), NW Africa and South America (Amazonia[2]) and to lesser extent Australia and India. At 250 Ma Gondwana stretched from the equator to the South Pole and slowly drifted northward whilst it experienced break-up from about 160 Ma, when East (India, Madagascar, Australia and Antarctica) and West (Africa, Arabia and South America) Gondwana separated.

In the sequence of reconstructions from 250 to 30 Ma we keep the SMEAN[3] 1% slow contour for the sub-African LLSVP (approximation of the PGZs) fixed (thick blue line in Figs. S2-5) while the continents are 'moved' over it according to our reconstruction parameters. A truly remarkable pattern is observed for the Gondwana continents since most 'anomalous' kimberlite locations are related to the Canadian shield (Fig. 1): At practically all times kimberlite eruptions took place near the 1% slow contour (see 250 Ma very good fit, 240 Ma good except Australia, 230 Ma very good, 220 Ma good, 200-140 Ma excellent, 120-30 Ma good fit but some kimberlites plot at some distance inside the 1% slow contour). We have also plotted reconstructed LIPs on the diagrams; these are always close to the 1% slow contour.

Supplementary References

1. Jelsma, H.A. *et al.* Preferential distribution along transcontinental corridors of kimberlites and related rocks of Southern Africa. *South African J. of Geology* **107**, 301-324 (2004).
2. Hayman, P.C., Kopylova, M.G. & Kaminsky, F.V. Lower mantle diamonds from Rio Soriso (Juina area, Mato Grosso, Brazil). *Contrib. Mineral. Petrol.* **149**, 430-445 (2005).
3. Becker, T.W. & Boschi, L. A comparison of tomographic and geodynamic mantle models. *Geochem. Geophys. Geosyst.* **3**, 1003, doi:10.1029/2001GC000168 (2002).
4. Castle, J.C., Creager, K.C., Winchester, J.P. & van der Hilst R.D. Shear wave speeds at the base of the mantle. *J. Geophys. Res.* **105**, 21543-21558 (2000).
5. Kuo, B.-Y., Garnero, E.J. & Lay, T. Tomographic Inversion of *SSKS* times for shear wave velocity heterogeneity in D": Degree 12 and hybrid models *J. Geophys. Res.* **105,** 139-157 (2000).
6. Torsvik, T.H., Steinberger, B., Cocks, L.R.M. & Burke, K. Longitude: Linking Earth's ancient surface to its deep interior. *Earth Planet. Sci. Lett.* **276**, 273-283 (2008).
7. Torsvik, T. H., Smethurst, M. A., Burke, K. & Steinberger, B. Large igneous provinces generated from the margins of the large low-velocity provinces in the deep mantle. *Geophys. J. Int.* **167**, 1447–1460 (2006).
8. Torsvik, T.H., Smethurst, M.A., Burke, K. & Steinberger, B. Long term stability in Deep Mantle structure: Evidence from the ca. 300 Ma Skagerrak-Centered Large Igneous Province (the SCLIP). *Earth Planet. Sci. Lett.* **267**, 444-452 (2008).
9. Haggerty, S.E. A diamond trilogy: superplumes, supercontinents, and supernovae. *Science* **285**, 851-861 (1999).
10. Eide, E.A. & Torsvik, T.H. Paleozoic Supercontinent assembly, Mantle flushing and genesis of the Kiaman Superchrons. *Earth Planet. Sci. Lett.* **144**, 389-402 (1996).
11. Gee, J.S. & Kent, D.V. in *Treatise on Geophysics, v.5, Geomagnetism* (Ed Kono, M.) 455-507 (Elsevier, Amsterdam, 2007).

12. England, P. & Houseman, G. On the geodynamic setting of kimberlite genesis. *Earth Planet. Sci. Lett.* **67**, 109-122 (1984).
13. Torsvik, T.H., Rousse, S., Labails, C. & Smethurst, M.A. A new scheme for the opening of the South Atlantic Ocean and dissection of an Aptian Salt Basin. *Geophys. J. Int.* 177, 1315-1333 (2009).
14. Torsvik, T.H., Müller, R.D., Van der Voo, R., Steinberger, B. & Gaina, C. Global plate motion frames: Toward a unified model. *Rev. Geophys.* **46**, RG3004, doi:10.1029/2007RG000227 (2008).
15. Parsiegla, N., Gohl, K. & Uenzelmann-Neben, G. The Agulhas Plateau: structure and evolution of a Large Igneous Province. *Geophys. J. Int.* **174,** 336-350 (2008).
16. van der Meer, D.G., Spakman, W., van Hinsbergen, D.J.J., Amaru, M.L. & Torsvik, T.H. Towards absolute plate motions constrained by lower-mantle slab remnants. *Nat. Geosci.*, **3**, 36-40, doi:10.1038/NGEO708 (2010).

Supplementary Table S1

Mean great circle distance in degrees (D ± 1σ) of reconstructed large igneous provinces (LIPs) and kimberlites from the 1% slow SMEAN contour and the number of LIPs and kimberlites erupted within a half-band of 10° from that contour (%W10°). We also calculate the corresponding values for the 0.96% slow contour in the CASTLE[4] and the 0.77% slow contour KUO[5] D" models. N = Number of LIPs/kimberlites.

Age intervals		SMEAN		CASTLE		KUO	
	N	D ± 1σ	%W10°	D ± 1σ	%W10°	D ± 1σ	%W10°
LIPs							
15-297 Ma	25	8 ± 9	80	5 ± 3	96	6 ± 4	88
Kimberlites (All)							
27-314 Ma	1395	12 ± 12	57	9 ± 7	73	7 ± 9	78
27-542 Ma	1588	11 ± 12	62	8 ± 7	76	7 ± 9	80
341-542 Ma	193	8 ± 4	93	5 ± 3	94	4 ± 5	90
Kimberlites (excluded North America/Canada)							
27-314 Ma	1156	7 ± 5	73	6 ± 4	85	3 ± 3	94
27-542 Ma	1349	7 ± 4	69	6 ± 4	86	4 ± 4	94

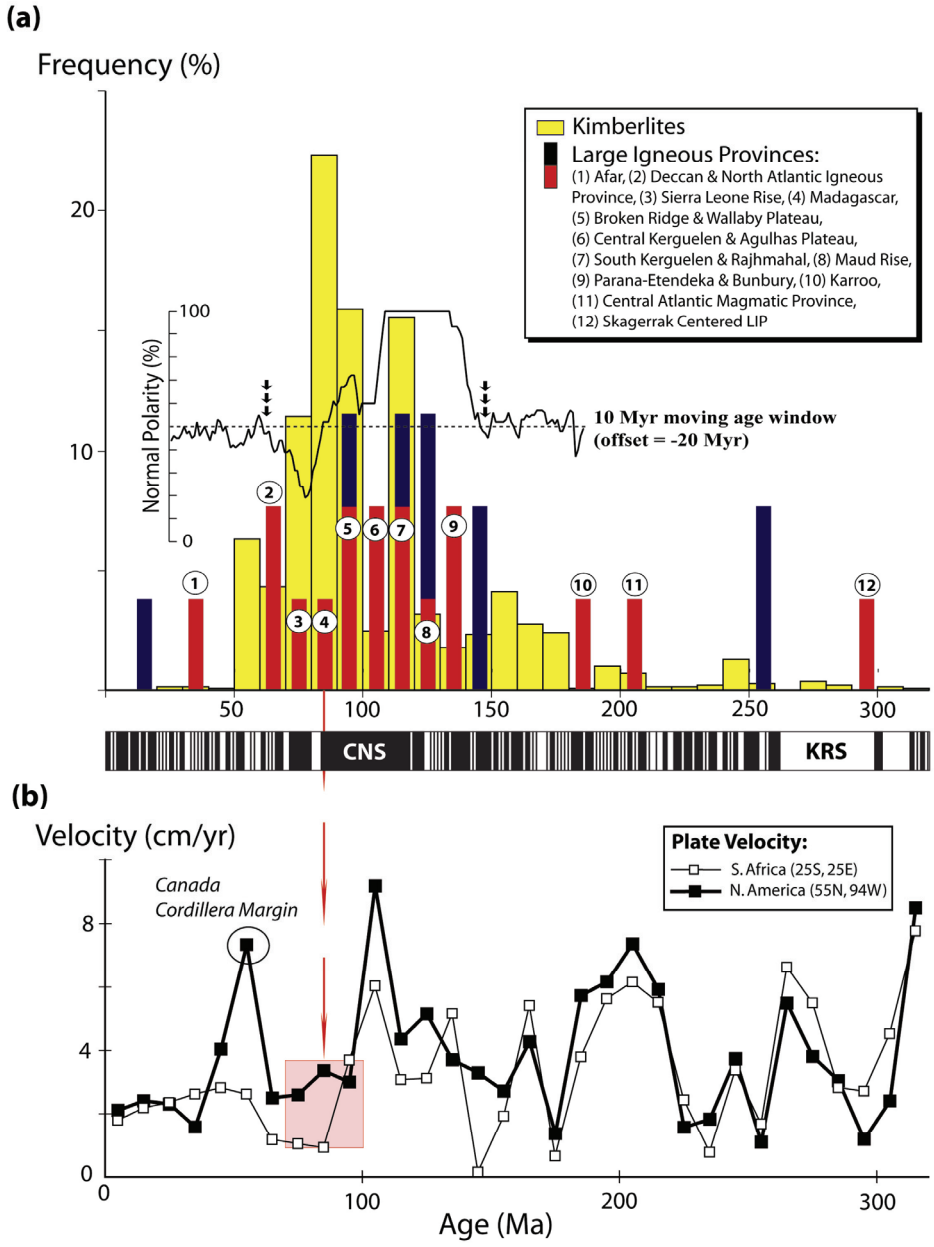

Figure S1 (Torsvik et al. 2010)

SUPPLEMENTARY FIGURE S1 (a) Frequency histogram in percentage for kimberlites (this study) and LIPs[6-8] vs. time (Ma) since the Carboniferous (320 Ma). LIPs with red shading are linked to the sub-African PGZ. A high frequency of kimberlites seems to be associated with or slightly younger than peak LIP activity. A link of LIP and kimberlite activity with the Earth's magnetic field has been postulated (e.g.[9]) and we show the magnetic polarity scale[10,11] since the Carboniferous. CNS = Cretaceous Normal Superchron (83.5-120.6 Ma); KRS = Kiaman Reverse Superchron. We also show a detailed analysis of the magnetic polarity pattern (expressed as percentage normal polarity) since the oldest M-anomaly (M29; ~157 Ma[11]). We smoothed the record using a 10 Myr sliding age-window

and show it with a 20 Myr offset (approximately the estimated time for a deep plume from the CMB to reach the surface). A normally reversing geodynamo is expected to have a ~50% normal polarity (stippled black line) but note that the polarity record shows a strong polarity bias (mostly normal, including the CNS but also a reverse bias in the Late Cretaceous-Early Tertiary). This polarity bias period lasted for ~90 Myr and coincides after applying the 20 Myr offset with the period between the start (Magellan and Shatsky Rise LIPs in the Pacific; 147-145 Ma surface eruption ages) and the end (Deccan and the North Atlantic Igneous Province LIPs; 65-60 Ma) of the most spectacular LIP (and Kimberlite) activity in Earth History.

(b) 'Absolute' velocities for South Africa and North America calculated for a central location for each continent (for comparison with England & Houseman[12] using the same values for 'center of gravity'). There is a notable low for South Africa between 80-90 Ma (pink rectangle) that corresponds to the maximum peak in kimberlite eruption activity. Velocity curves for South Africa and North America are essentially similar before 180 Ma when they both were part of Pangea.

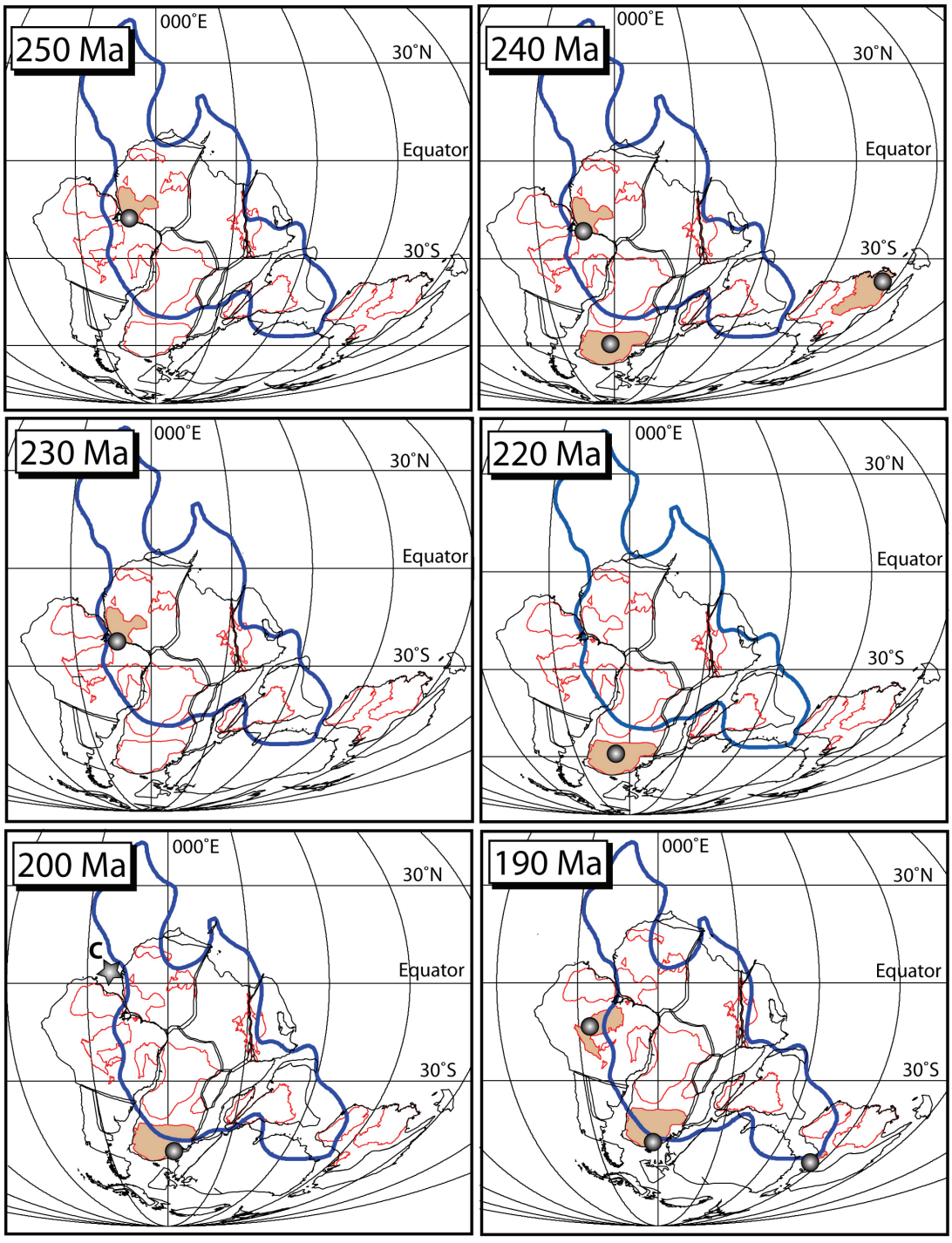

Figure S2 (Torsvik et al. 2010)

SUPPLEMENTARY FIGURE S2 Reconstruction of Gondwana continents and associated kimberlites and old cratons (shaded colour) in space and time. Kimberlite symbols (grey circles) normally represent multiple kimberlite eruption sites. The 1% slow contour (SMEAN model) is shown as a thick blue line in all diagrams. C=Central Atlantic Magmatic Province (~200 Ma). Kimberlites (and LIPs) are plotted if they are within ± 5 Myr of the actual reconstruction age. There are no known Gondwana kimberlites or LIPs at 210 ± 5 Ma. Details in the break-up history between Africa and South America and intra-plate deformation are based on Torsvik et al.[13]. Other relative fits are listed in Torsvik et al.[14]

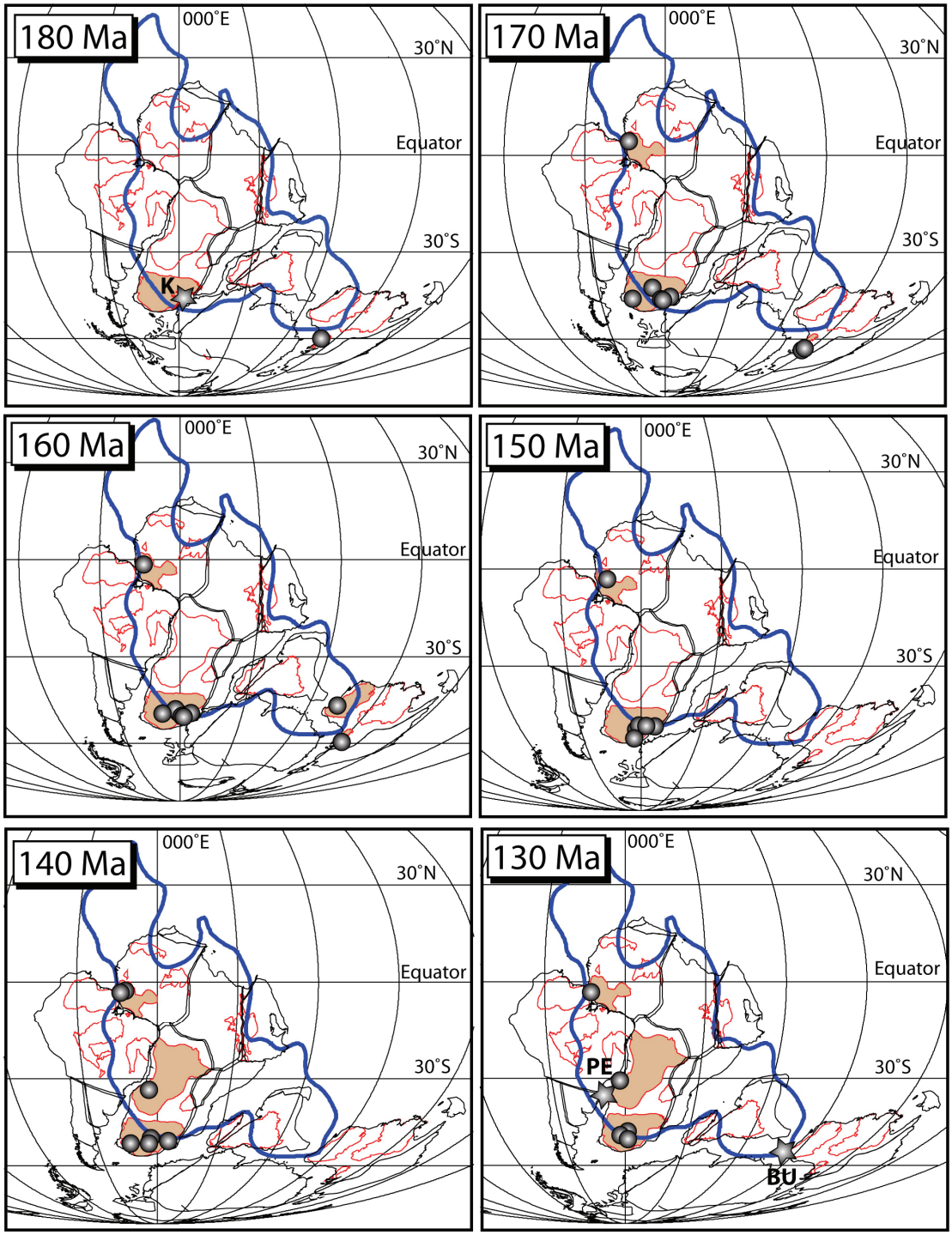

Figure S3 (Torsvik et al. 2010)

SUPPLEMENTARY FIGURE S3 See figure S2 caption. K=Karroo LIP (c. 182 Ma); PE=Parana-Etendeka LIP (~132 Ma); BU=Bunbury (~132 Ma).

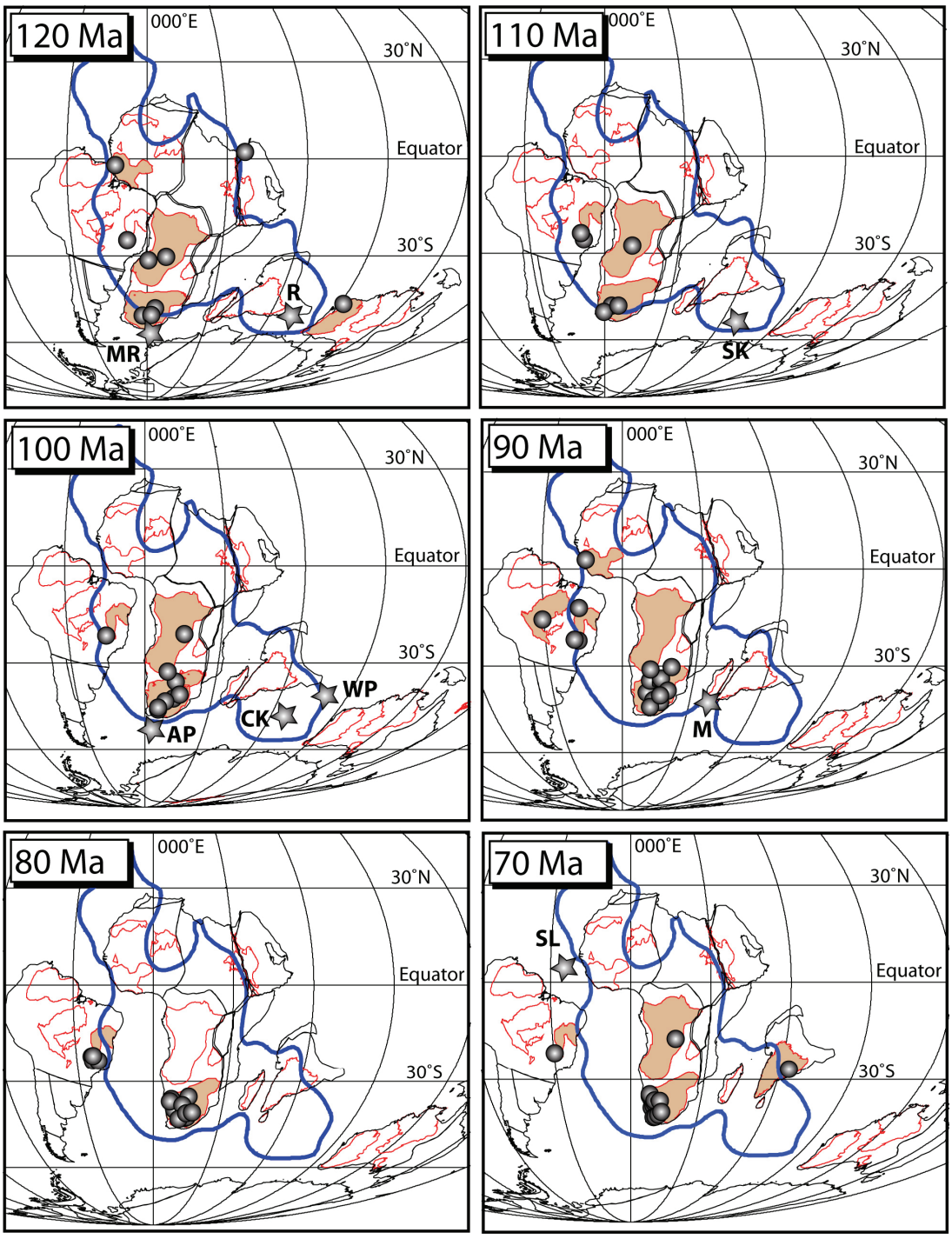

Figure S4 (Torsvik et al. 2010)

SUPPLEMENTARY FIGURE S4 See figure S2 caption. R=Rajmahal LIP (~118 Ma); MR=Maud Rise LIP (~125 Ma); SK=South Kerguelen (~114 Ma); CK=Central Kerguelen (~100 Ma); WP=Wallaby Plateau (~96 Ma); AP=Agulhas LIP (~100 Ma[14,15], M=Madagascar-Marion (~87 Ma); SL=Sierra Leone (~73 Ma)

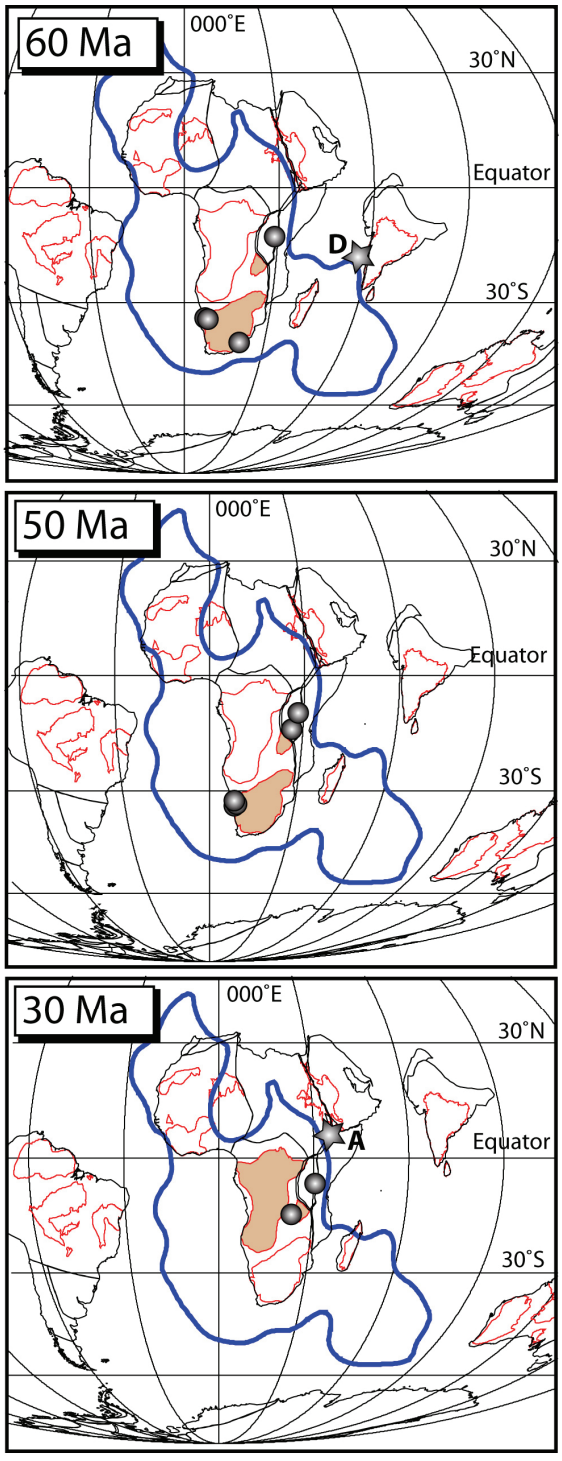

Figure S5 (Torsvik et al. 2010)

SUPPLEMENTARY FIGURE S5 See figure S2 caption. D=Deccan Trap LIP (~65 Ma); A=Afar LIP (~31 Ma).

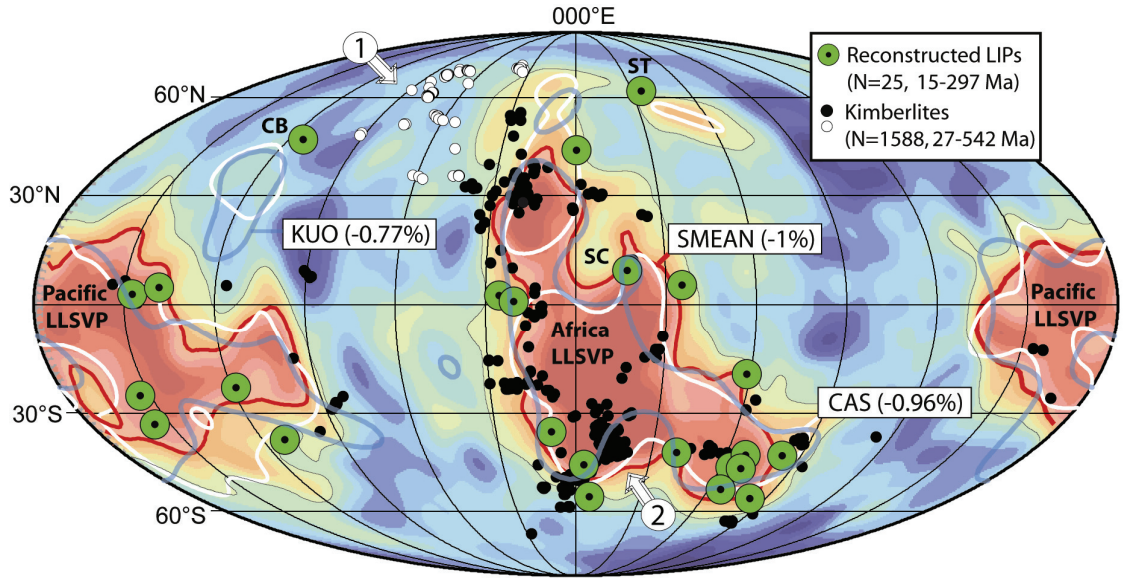

Figure S6 (Torsvik et al. 2010)

SUPPLEMENTARY FIGURE S6 Reconstructed large igneous provinces and kimberlites for the past 542 Myr with respect to shear-wave anomalies at the base of the mantle (2800 km on the SMEAN tomography model[3]). This figure combines Figures 1 and 4, and in addition we compare the 1% slow SMEAN contour (red colour) with the 0.96% slow contour of the Castle et al.[5] (white colour) and the 0.77% slow contour of the Kuo et al.[6] (blue colour) D" models. The latter show a sharper bend along the SW margin of the African LLSVP and therefore many Cretaceous kimberlites from South Africa, which form a large cluster that dominates the kimberlite record, will better fit this contour. For guidance we also show the zero contour of the SMEAN model (thin black line). Anomalous kimberlites (Late Cretaceous-Early Tertiary kimberlites from North America/Canada, white dots) are indicated by white arrow 1 whilst an area of Cretaceous kimberlites from South Africa plotting at some distance inside both the SMEAN and CASTLE contour but directly above the KUO contour are indicated by white arrow 2. Annotated reconstructed LIPs are: CB=Columbia River Basalt (15 Ma), ST=Siberian Traps (251 Ma), SC=Skagerrak Centered LIP (297 Ma; the oldest reconstructed LIP).

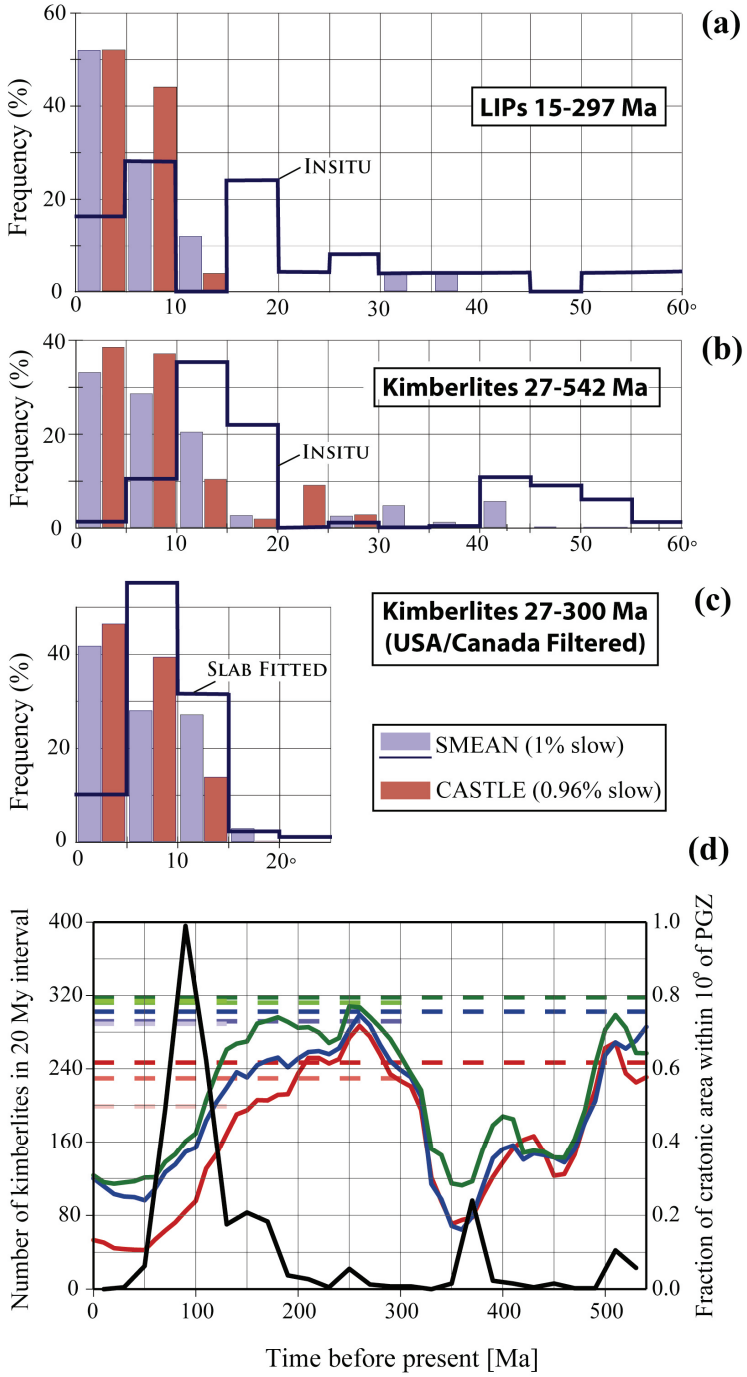

Figure S7 (Torsvik et al. 2010)

SUPPLEMENTARY FIGURE S7 Calculated great circle distances of reconstructed LIPs **(a)** and all kimberlite **(b)** eruption sites from the 1% slow SMEAN contour (blue histograms) and the 0.96% slow CASTLE contour (red histogram). Histograms were binned in 5 Myr intervals. We also show the histogram distribution for *in-situ* locations (i.e. present sampling sites) vs. the SMEAN contour (blue lines). In **(c)** we have excluded the anomalous Late Cretaceous-Early Tertiary North American kimberlites and compare two tomography models and two different plate models (our hybrid model compared with the slab fitted model[16]). In essence **(a)** to **(c)** show that reconstructed eruption sites cluster near the SMEAN contour

much better than in-situ sites, the CASTLE model actually provides an improved fit and our plate model compares favourably with the slab-fitted model. **(d)** The red, blue and green curves are the fraction (right scale) of cratons that are within 10° of the SMEAN 1%, CASTLE 0.96% and KUO 0.77% slow margin as a function of time in 10 Myr intervals. The black curve gives the age distribution (number of kimberlites – left scale - binned in 20 Myr intervals, plotted at the centre age of the bin). Dashed lines show for comparison the fraction of kimberlites that erupted within ± 10° of the PGZs. Dark colour is for all kimberlites erupted since 542 My, lighter colour for all kimberlites erupted since 320 My, lightest colour since 130 My. The plot would look very similar for 15° instead of 10°, with both dashed and continuous coloured lines somewhat raised.

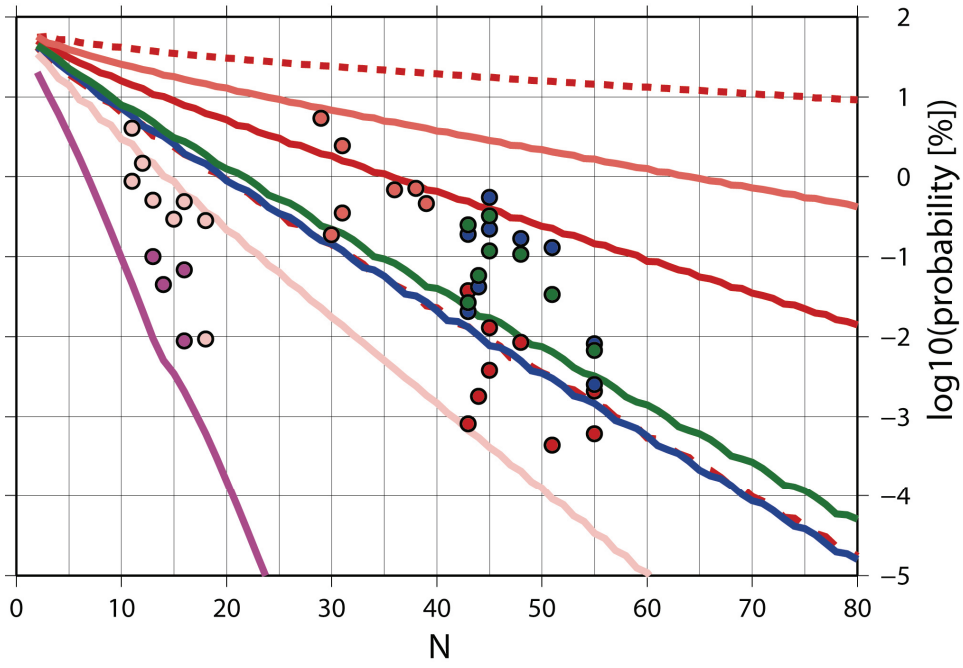

Figure S8 (Torsvik et al. 2010)

SUPPLEMENTARY FIGURE S8 Probability that the distribution of kimberlites (dashed and continuous lines; filled circles) and cratons (dotted lines) relative to the PGZs arises by chance, computed under different assumptions. In each case, we address the following question: if the probability for an outcome (e.g., rolling a six with a dice, or – in this case - the eruption of a kimberlite within 10° of the PGZ) is p_1 , what is the probability that this outcome occurs $p_2 \cdot N$ or more out of N times? But whereas each rolling of a dice can be viewed as statistically independent, this is certainly not the case for eruptions of kimberlites. We address the problem of appropriately estimating N in two ways: Firstly (plotted as lines), we leave N as a free parameter, and use for p_2 the fraction of individual kimberlites within 10° of the PGZ. If $p_2 \cdot N$ is non-integer, it is rounded up to the nearest larger integer, but resulting fluctuations are subsequently smoothed. For red, pink and violet lines, the -1% SMEAN contour defines the PGZ. The dashed line (partly hidden behind the blue line) indicates the probability that the fraction p_2 is as large as observed (980 out of 1588 kimberlites since 542 Ma), or even larger, if they are placed randomly on the surface of the sphere: Hence we use

p_1=33.1% (fraction of the Earth's surface within 10° of the PGZs) and p_2=980/1588=61.7 %. For comparison, the dotted line indicates the probability that the fraction of *cratons* within 10° of the PGZ is as large as observed or larger, if cratons are distributed randomly on the surface of the sphere: Hence we use again p_1=33.1%, but p_2=40.8 % (time-averaged fraction of cratons within 10° of the PGZs; see Fig. S7d). The dotted line shows that cratons can be considered as distributed randomly relative to PGZs. In contrast, the continuous red line indicates the probability that the fraction of kimberlites erupting within 10° of the PGZ is as large as observed or larger, if they are placed randomly in space and time *on the cratons*. Hence we use here p_1=40.8 % and p_2=61.7 %. While the (dark) red lines are for *all* kimberlites, the medium light red (pink) line is restricted to the past 320 Myr (p_1=42.1%, p_2=57.4% - 801 of 1395), the time after Pangaea assembly for which we have better constraints in longitude. The light red (pink) line is for the past 130 Myr (p_1=18.9%, p_2=49.5% - 570 of 1151) for which we have hotspot tracks in the African hemisphere and thus the best constraints in longitude. The violet line is for times before 320 Ma (p_1=38.9%, p_2=92.7% - 179 of 193). For the blue line, the -0.96% CASTLE[20] contour defines the PGZ (p_1=46.7%, p_2=75.6%), for the green line, the -0.77% KUO[21] contour (p_1=52.3%, p_2=79.5%). Blue and green lines are again for all kimberlites since 542 Ma. Secondly (plotted as dots; same color scheme), we divide the kimberlites into groups that are then regarded as statistically independent: We group one kimberlite with another one if it is less than 15° away with less than 30 My age difference, and average latitude, longitude and age within the groups. The grouping somewhat depends on the order of going through the set of kimberlites. whether (a) from beginning to end, (b) in reverse order, or (c) in random order (two cases; www.random.org/sequences/). In each case, we iterate the grouping until the number of groups remains constant. In this way, we obtain nine sets of 43-55 groups, if we consider all kimberlites since 540 Ma, nine sets of 29-39 groups since 320 Ma, nine sets of 11-18 groups since 130 Ma and seven sets of 13-16 groups before 320 Ma. Since the number of kimberlites per group strongly varies (between 1 and 380-726) the fraction p_2 for groups can be quite different from the fraction for individual kimberlites, whereas we use the same p_1 values as for the continuous lines. Hence corresponding dots and lines can be quite apart.